AIP Advances

New Cf-252 neutron source shielding design based Monte Carlo simulation using material combination

Cite as: AIP Advances **10**, 075203 (2020); https://doi.org/10.1063/1.5144923
Submitted: 12 January 2020 . Accepted: 08 June 2020 . Published Online: 01 July 2020

Cebastien Joel Guembou Shouop, Sang-In Bak, Maurice Ndontchueng Moyo, Eric Jilbert Nguelem Mekongtso, and David Strivay

COLLECTIONS

Paper published as part of the special topic on Chemical Physics, Energy, Fluids and Plasmas, Materials Science and Mathematical Physics

New Cf-252 neutron source shielding design based Monte Carlo simulation using material combination

Cite as: AIP Advances 10, 075203 (2020); doi: 10.1063/1.5144923
Submitted: 12 January 2020 • Accepted: 8 June 2020 •
Published Online: 1 July 2020

View Online Export Citation CrossMark

Cebastien Joel Guembou Shouop,[1,2,3,a] Sang-In Bak,[4] Maurice Ndontchueng Moyo,[2,5] Eric Jilbert Nguelem Mekongtso,[2,5] and David Strivay[3]

AFFILIATIONS

[1] Korea Advanced Institute of Science and Technology—KAIST, 291, Daejeon 34142, South Korea
[2] National Radiation Protection Agency of Cameroon, Box 33732, Yaounde, Cameroon
[3] Atomic and Nuclear Spectroscopy, Archeometry, University of Liège, Bat. B15 Sart Tilman, 4000 Liege 1, Belgium
[4] Korea Institute of Nuclear Safety (KINS), 62 Gwahak-ro, Yuseong-gu, Daejeon 34142, South Korea
[5] UFD Mathématiques, Informatique Appliquée et Physique Fondamentale, Université de Douala, P.O. Box 24157, Douala, Cameroon

[a] **Author to whom correspondence should be addressed:** sebastianguembou@gmail.com

ABSTRACT

Neutron shielding has been a worldwide concern for decades and appropriate methods in nuclear reactors and associated facilities for shielding have been developed. Light materials such as paraffin and water cannot be used in neutron radiography due to structural and fire concerns, and a material in the solid form is needed for effective neutron shielding. Therefore, the present study developed a new neutron shielding design for fixed industrial radiography facilities with solid structures based on material combination. Different materials were investigated to find the most appropriate combination design to shield the spontaneous neutron emitted from a Cf-252 source (with an energy in the range from several keV up to 20 MeV). The combination of iron, graphite, boron (or borate materials), and lead in this order, respectively, were found to be the most appropriate shielding structure for an open Cf-252 source used in fixed industrial radiography. As iron is characterized by a high removal cross section, its use in shielding the californium spontaneous neutron source is the key outcome of the present study. These results were confirmed with the Monte Carlo simulation-based particle and heavy ion transport code system.

I. INTRODUCTION

Recently, neutron radiography steadily developed and its applications include a wide range of verification processes. Because neutrons easily penetrate heavy materials such as steel, lead, depleted uranium, and other important materials used for equipment manufacturing, their utilization for radiography is complementary to that of gamma and x rays (photons). In addition, neutrons are absorbed by hydrogenous material, boron and borate materials, and plastics (light elements). Even though they provide a useful insight for radiography, a real concern about the appropriate shielding and effective neutron moderator has been subjected to investigation and studies for decades. Radioisotopes considered as neutron sources include a single radioisotope, Cf-252, and combine radionuclides for alpha-neutron or gamma-neutron generation (Am/Be, Li/Be, ...). The isotope Cf-252 of californium is one of the most intense neutron emitters with a high flux that can reach 2.314×10^{12} s^{-1} g^{-1}.[1–5] Cf-252 finds many neutron applications in physics, research, and industry. However, it poses nuclear and radiation safety concerns while in use, as the neutron shielding is not easily achieved and is compromised by economic impact and structural factors.

Neutron shielding has been identified as a major concern in the neutron industry and the suggested solutions are always under optimization.[3,5–10] Different materials have been developed to achieve the effective attenuation of neutrons in the nuclear reactor, accelerator-based spallation, and industrial application as radiography (non-destructive testing). Materials such as boron, borate material, lithium, water, hydrogenous materials, graphite, and other low Z materials were used for neutron shielding and protection. However, difficulties were encountered during the development and construction of infrastructures for neutron imaging: the structural problems do not allow the use of water as shielded enclosures around the Cf-252 source. The use of plastic or paraffin is subjected to fire protection and involved additional technical applications. Neutron properties differ from photon properties that the attenuation law is Z-dependent. In addition, borate materials, lithium, and other composite materials were found to be economically not recommendable for some applications (as NDT testing).

The present study aims to develop a new and efficient shielding design for neutrons emitted from a Cf-252 spontaneous fission source based on the material's combination. As iron and boron could be used to slow neutrons down and absorb them, respectively, the use of a combined material and their arrangement in the installation design is a key outcome of the present study. The solution developed during the present research project was an extension of neutron shielding based Monte Carlo simulation.[11,12] The Particle and Heavy Ion Transport code System (PHITS) was used for computation.[13–18] Different materials were set up with an order to optimize the total removal cross section for neutrons based on cost-benefit evaluation in the NDT industry. This manuscript describes the simulation arrangement, the result obtained, and the discussion based on the interpretation of the output of the simulation.

II. SIMULATION

A. Monte Carlo code PHITS

Monte Carlo (MC) techniques are usually defined as a subset of computational algorithms that utilize the process of repeated random sampling to numerically estimate unknown parameters. They are used to model complex situations and problems with a high degree of freedom by generating random numbers and random

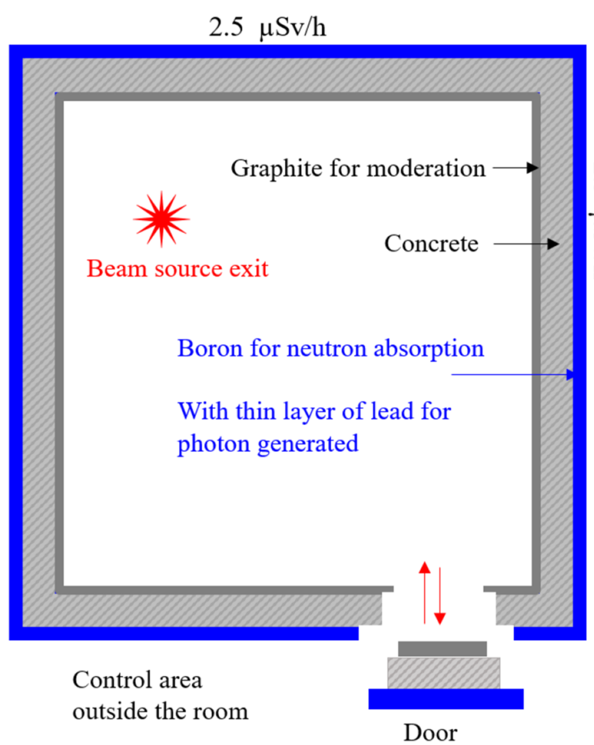

FIG. 1. Design for industrial neutron radiography installation including a neutron source, walls with different materials combination, and the main door (access) position and design. The door is different from that used in gamma radiography and maze design is ineffective as a reinforced door in this design.

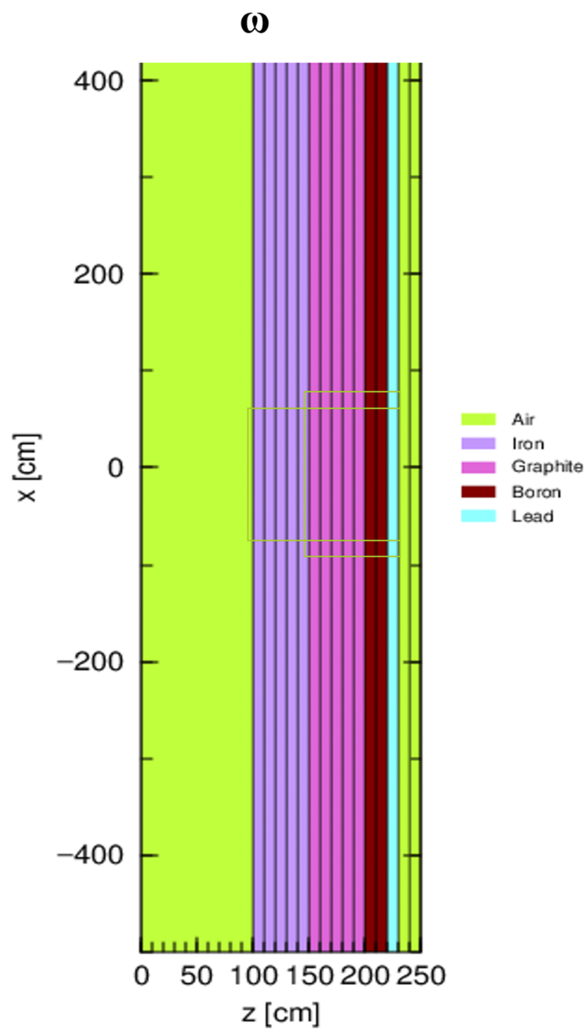

FIG. 2. Facility (walls as set of concrete in Fig. 1) design for neutron shielding and system arrangement for effective material selection. ω is a 50 cm layer of either graphite, paraffin, and iron.

experiments. The Particle and Heavy Ion Transport code System (PHITS) was used for simulation in the present research. It is a general-purpose Monte Carlo system based on Fortran code. The PHITS version 3.10 was used for computation, including the simulation of photons and neutrons in a wide range of energy. The code developed was executed in shared-memory parallel computing using supercomputers (clusters). It is used in applications such as computer science, nuclear data evaluation, nuclear reaction model, human modeling, induced activity, facility design, medical physics, radiation protection, geoscience, etc.[19,20] Its use for shielding design and radiation protection requires proper material definition and geometry construction following a clear and well-defined method. The parameter set for uncertainties calculation in the present project was based on the following equation:

$$\sigma = \sqrt{\frac{\sum_{i=1}^{N}\left(x_i w_i \big/ \bar{w}\right)^2 - N\bar{X}^2}{N(N-1)}}. \tag{1}$$

The PHITS input code was executed using the radioactive decay process, a data library from DECDC2 (Nuclear DECay Data for Dosimetry Calculation, Version 2) revised data from ICRP Publication 38. This library has been compiled for 1034 radionuclides for dose calculation in medical, environmental, and occupational exposures. It is a library built from the assembled set of Evaluated Nuclear Structure Data File (ENSDF).

B. Fundamental basis

Neutron interaction with a medium is known as a function depending on cross sections. If a neutron interacts with a light particle or nucleus, the probability of interaction is known as microscopic cross section (σ), expressed in barn or cm^2 and the probability of interaction with heavy materials such as a wall, concrete, compound, is known as the macroscopic cross section. The total interaction cross section of neutrons entering a medium in our simulated geometry is the summation of all cross sections including scattering, absorption, capture, fission, etc.[9] The macroscopic cross section is then expressed by the following equation:

$$\Sigma = N\sigma, \tag{2}$$

$$\Sigma_{Total} = \Sigma_{Scattering} + \Sigma_{Absorption} + \Sigma_{Capture} + \Sigma_{Fission} + \cdots, \tag{3}$$

$$N = \frac{\rho}{A} N_A, \tag{4}$$

where N is the atomic density of the target material, ρ the density of the target material, and N_A Avogadro's number. Materials with large total cross section are good neutron moderators even though the important parameter to be considered physically is the removal cross section.

Another important parameter in neutron shielding is the mean free path λ, the average distance a neutron particle travels between two collisions in the target material. The collisional probability at a distance dx taken by a neutron in a medium is computed using the following relations:[9]

$$p(x)dx = \sum_t dx \cdot e^{-\Sigma_t} \cdot x = \sum_t e^{-\Sigma_t} \cdot x \cdot dx, \tag{5}$$

$$\lambda = \int_0^{\infty} p(x) \cdot x \cdot dx = \frac{1}{\Sigma_t}, \tag{6}$$

where λ is the distance that neutrons can travel in the target material without interaction. Neutron transmission number of incoming and passing neutrons determine the properties of materials used

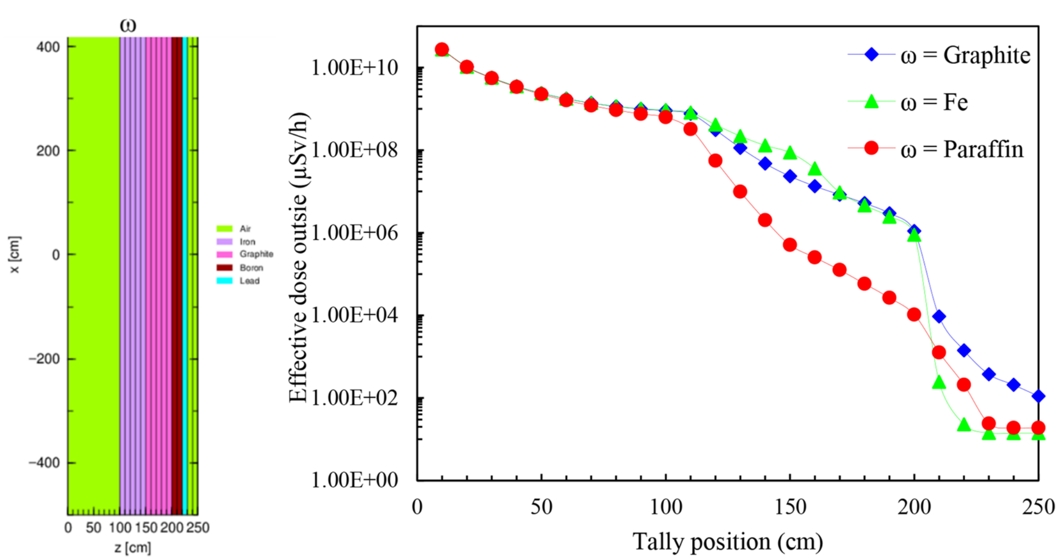

FIG. 3. Investigation of the impact of three important moderators related to the Cf-252 spontaneous source. Discussion on the case of graphite, iron, and paraffin and their effects on shielding design.

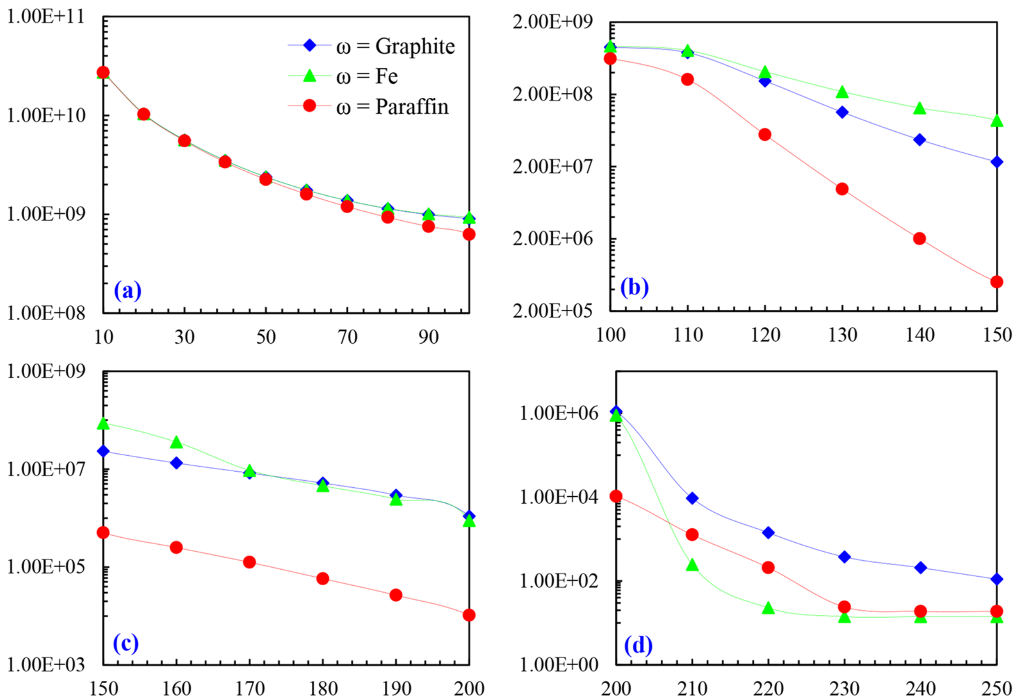

FIG. 4. Investigation of the impact of three important moderators related to the Cf-252 spontaneous source. Differentiation of different sections or layers of the shielding material used in the shielded enclosures as the geometry is based on material combination. Results of graphite, iron, and paraffin: (a) represents the result of the interior of the facility made of air. (b) represents the result in the 50 cm of graphite, iron, or paraffin. (c) represents the result in the following layer made of 50 cm graphite. (d) represents the result in 20 cm borate material, 10 cm lead, and 20 cm air set as tally for decision making on effective dose rate computation, outside the shielding enclosures.

and its ability to slow down neutrons or absorb them. The PHITS code was used to determine the effectiveness of material combination in slowing down and absorbing neutron in a facility.[15,19,21] That ability is related to the distance λ and the removal cross section.

III. MATERIAL AND METHODS

The equipment consisted of a Cf-252 spontaneous neutron source, disposed of in a room built for fixed neutron radiography purposes. The source consisted of 100 Ci Cf-252 in a closed facility and the computation included geometry simplifications by allowing interaction with only one wall in the first step and with the full geometry in the second step. The room is filled with normal air at atmospheric pressure, surrounded by enclosure walls built with different layers of shielding materials. The description of the geometry is given in Figs. 1 and 2. As the spontaneous neutrons produced by a Cf-252 source are mostly fast neutrons, moderation is a key process to slow down fast neutrons prior to their absorption in the absorbent material. The layer considered as concrete in the geometry presented in Fig. 1 is finally made of a material presented in the geometry described in Fig. 2.

The first element set in the geometry could play the role of the filtering (slowing down or removal of very fast neutrons) material and the second 50 cm layer set is graphite, and the third layer is boron for neutron absorption. The fourth layer in the geometry is a 10 cm layer of lead. The tally for dose calculation is set in the normal area to the source and the tally for decision making is in the last 10 cm of air in the area adjacent to the radiography room. This

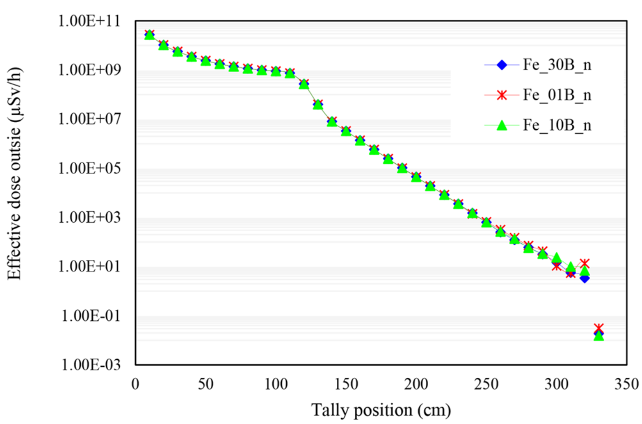

FIG. 5. Statistical variation depending on the numbers of particles run in the PHITS code. Three different numbers of particles were run for the same geometry and the difference is shown only in the last tallies.

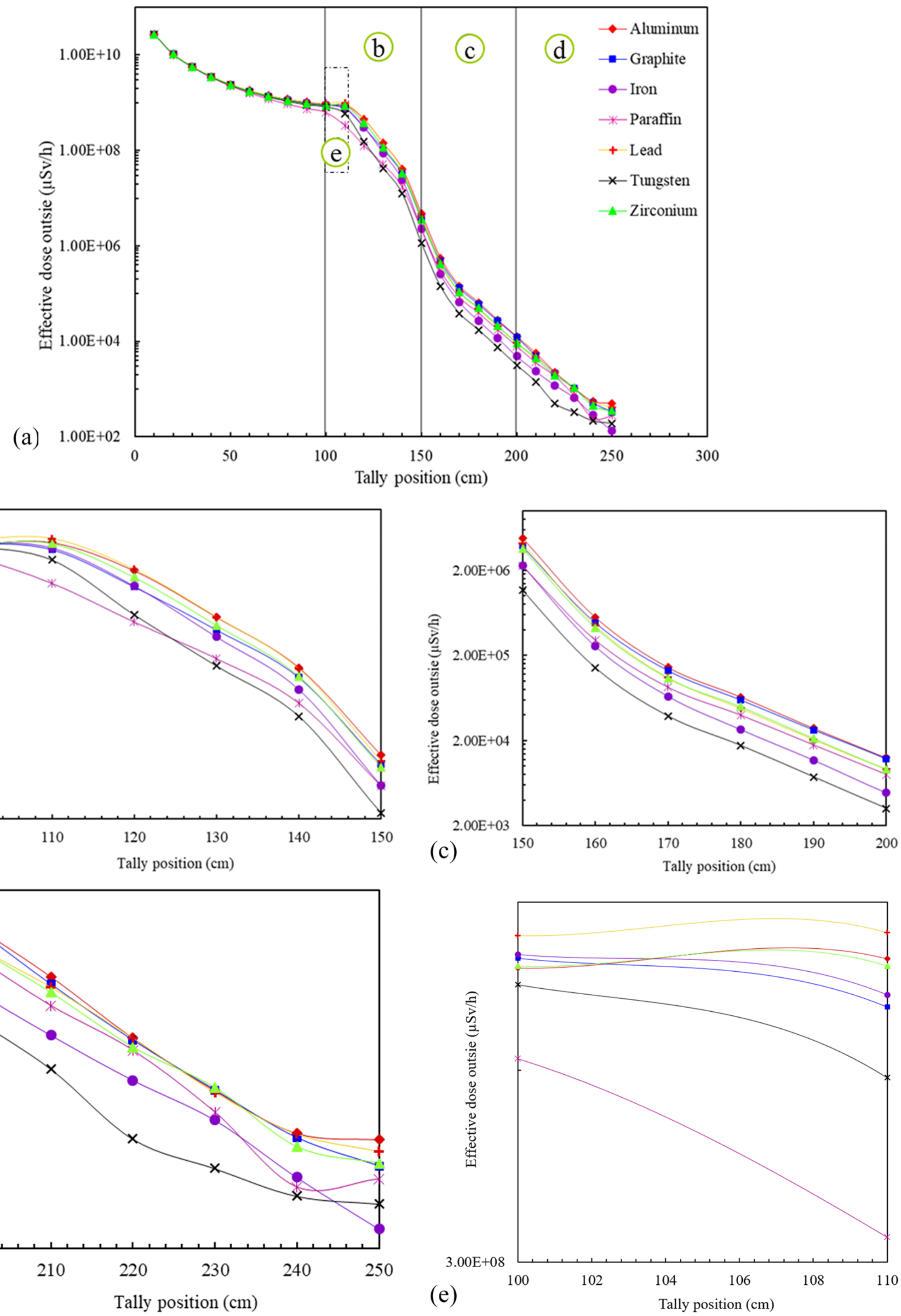

FIG. 6. (a) Preliminary results of the dose calculation in the geometry in the tally set for computation. All materials used as the first layer in the previous described geometry are displayed here. The first 100 cm layer represents the air in the imaging room and different material properties are observed in the layer between 100 cm and 250 cm. (b) Result of lead, iron, graphite, aluminum, tungsten, zirconium, and polyethylene in the first layer (10 cm) of the geometry (100 cm–110 cm) followed by 30 cm of graphite and 10 cm of boron or borate material. (c) Impact of lead, iron, graphite, aluminum, tungsten, zirconium, and polyethylene in the first layer of the geometry on the mid-part of the geometry (150 cm–200 cm) made of 10 cm of boron or borate material and 40 cm of concrete. (d) Impact of lead, iron, graphite, aluminum, tungsten, zirconium, and polyethylene in the first layer of the geometry on the later part of the geometry (200 cm–250 cm) made of 20 cm of concrete, 10 cm of lead, and air for kerma or effective dose computation. (e) Lead, iron, graphite, aluminum, tungsten, zirconium, and polyethylene results as the result of the first layer of the geometry impact (150 cm–160 cm).

arrangement was made of the most conservative case in such facilities for dose assessment. The computation was done by running at least one billion (10×10^9 or more) neutrons for each case and the relative standard deviation for all the presented results (effective for decision making) is less than 5%. Difficulties were encountered for statistics, as the result obtained showed a large standard deviation for the deep target material, especially in the latest tally for decision-making on dose rate computation.

IV. RESULTS AND DISCUSSIONS

The shielding results obtained are presented in Figs. 3–5. The overall result of Monte Carlo simulation is described in Fig. 3 with detailed explanations from layer to layer in Fig. 4. The first 100 cm layer in the geometry made of air at atmospheric pressure and with ambient temperature showed negligible attenuation of neutrons. Their range in air is a few hundred meters, and for this reason, 1 m of air is considered too small to impact the attenuation and transmission of neutrons crossing the geometry. An important characteristic of graphite is to moderate neutron with energy up to 2 MeV–5 MeV. However, the energy spectrum of Cf-252 has energy ranges from several keV up to 20 MeV. There is a range of energy from 2 MeV–5 MeV to 20 MeV that cannot be effectively slowed down by graphite and the effect can be seen on the blue and red curves. The absorption is really effective, but the slowing down process was inefficient and the fast neutrons easily reach the external layer of the geometry. Neutrons with a low energy are quickly slowed down and the flux is reduced drastically in the borate material layer, especially in the boron (or borate material) layer. Attention should though be paid on the range of energy at which neutron reaches the borate material layer.

The effect of iron on the shielding of neutrons from Cf-252 is the most important and effective. The curve is complex as the iron's effect is not directly reflected in the first layer of the shielding, but it is the most effective case as the dose calculation in the tally outside the room shows a lower dose rate. The removal cross section of iron is higher than that of all other materials (except the case of water). In reality, neutrons with an energy above 2 MeV–5 MeV are not effectively slowed down by graphite as by iron, but below 2 MeV–5 MeV, graphite is really effective. Iron effectively slows-down neutrons with an energy above 2 MeV–5 MeV and the following graphite layer thermalizes them. When they reach the absorber (borate material), they are low-energy neutrons and the absorption process is more effective in the layer between 200 cm and 220 cm (boron layer), as shown by the curve in Figs. 3 and 4. The concept of shielding neutron above 2 MeV–5 MeV is a complex task as the mathematical function describing the interaction cross section of such neutrons is not linear. The effect of iron in the very early geometry is efficient and its combination in the geometry shows effective neutron shielding properties for the designed installation. It is drawn from this observation that the material order disposition for shielding purposes in a neutron radiography facility should be set in such a way that they work effectively.

So the overall filter in the case of graphite is effective for neutrons with an energy below 2 MeV–5 MeV. Neutrons with the energy above (as shown in the Cf-252 spectrum) are not slowed down effectively and their contribution in the later part of the geometry leads to a high dose rate. In this regard, neutrons reaching the boron layer (or borate material) are not thermalized and the absorption is less effective than the case where iron is used. The paraffin case is similar to that of graphite with the difference that it is effective than graphite (this is due to its hydrogenous composition). This was expected as its content in the hydrogenous material is considerable. Between 200 cm and 220 cm, the layer of boron inserted in the shielded enclosures is efficient as the neutron absorption is almost 10^6 times effective, especially for neutrons coming from iron, paraffin, and graphite, respectively. In addition, it is important to conclude that the most effective material to shield neutron in a facility used for neutron industrial radiography with fast spontaneous neutron from Cf-252 is the combination of a reasonable iron layer, followed by a graphite layer for effective moderation, a boron or borate material layer for neutron absorption, and a lead layer for gamma shielding[22] as the neutron interaction generates gamma. The three investigated materials (graphite, iron, and paraffin) were selected from the investigation of seven different materials and many combinations and their results are not presented here.

The previous results are based on the selection of three materials from seven, as presented in the following graphs [Figs. 6(a)–6(e)]. From 100 cm (the position of the shielding material, as the source is placed at least 100 cm away from the walls, doors, and all enclosures), the material effect on neutron transmission is evident, as described in different graphs. As can be seen in the figures, materials such as lead, aluminum, and zirconium were not as effective as tungsten, iron, and paraffin. From 100 cm to 110 cm, three materials were not really effective (lead, zirconium, and aluminum), as can be observed in Fig. 6(b). This is the reason why these materials were not considered in the previous major results presented. The most effective in this range are paraffin, tungsten (expensive), graphite, and iron, respectively. From 110 cm and above, all curves were the results of calculation for the same material composition and geometry arrangement.

It was thus recommended to use either paraffin, iron, or graphite for the first inside wall layer in the shielding design of a facility using Cf-252 for industrial radiography with high energy neutrons. The shielding enclosure took into account paraffin, graphite, or iron in the results described previously. The case of tungsten is not presented as it is not economically acceptable to be used in a shielding facility at a large scale. Tungsten is usually used to shield and collimate the beam of radiation confined in small geometries (the source itself, not an entire facility).

V. CONCLUSIONS

A new shielding design for the spontaneous Cf-252 neutron source based on material combination was developed based on Monte Carlo simulation. The PHITS Monte Carlo code was effective for dose rate computation. The idea was drawn from industrial radiography using a spontaneous neutron source of Cf-252 with a maximum activity of 100 Ci. Different material combinations were displayed and the most appropriate arrangement was found to be the combination of iron and graphite for neutron moderation in this order, respectively. This combination should be followed by a layer of boron or borate material for the absorption of neutrons that have been slowed down from the previous layer. The geometry ended with a thin layer of lead for gamma shielding as neutron interaction with a target material always produces secondary particles mostly made of gamma radiation. Graphite alone combined with a neutron absorber cannot achieve effective neutron moderation and absorption as that achieved while combining with iron (for Cf-252 source). Even plastic, paraffin, or other hydrogenous materials are effective for neutrons with energy lower than 2 MeV–5 MeV, iron is effective for removing neutrons with energy above 2 MeV–5 MeV, and the graphite layer set after iron plays an effective role in slowing down neutrons with an energy lower than 2 MeV.

The obtained results based on Monte Carlo simulation showed a clear description of the appropriate shielding design. As the geometry of calculation was simplified, future work will be shared about the implementation of the obtained result in neutron industrial radiography using the Cf-252 spontaneous source. The calculation will be done using the GEANT4 toolkit[23] and implementing the skyshine and floorshine phenomena and compared to PHITS code.[18,24]

SUPPLEMENTARY MATERIAL

See the supplementary material section for the description of the major data obtained in the project. It consists of two tables that present the data and four figures that explain the design process used to obtain data. This section is useful for the full understanding of the manuscript and the procedure used to select the main material investigated and presented in this study.

ACKNOWLEDGMENTS

The authors are grateful to the PHITS Collaboration (T. Sato, S. Hashimoto, K. Niita *et al.*) for PHITS development, to Korea Advanced Institute of Science and Technology—KAIST NQE Department (Y. Kim, J. Park, C. M. Choi *et al.*) for code license, and to Korea Institute of Nuclear Safety—KINS (Computer Lab). They want to extent their gratitude to the National Radiation Protection Agency of Cameroon—NRPA.

All authors have no conflict of interest to declare.

DATA AVAILABILITY

The data that support the findings of this study are available within the article and its supplementary material.

REFERENCES

1. H. Barros, E. D. Greaves, and H. R. Vega-Carrillo, "Graphite moderated ^{252}Cf source," Appl. Radiat. Isot. **100**, 108–112 (2015).
2. R. Gheisari and H. Mohammadi, "Assembly neutron moderation system for BNCT based on a ^{252}Cf neutron source," Prog. Med. Phys. **29**, 101 (2018).
3. H.-Y. Kang, C.-J. Park, K.-S. Seo, and J.-S. Yoon, "Evaluation of neutron shielding effects on various materials by using a Cf-252 source," J. Korean Phys. Soc. **52**, 1744–1747 (2008).
4. F. Abu-Jarad, "The application of radiation sources in the oil and gas industry and shortages in their services," At. Peace **2**, 4 (2009).
5. S. Alhajali, S. Yousef, and B. Naoum, "Appropriate concrete for nuclear reactor shielding," Appl. Radiat. Isot. **107**, 29–32 (2016).
6. D. H. Kim, C.-S. Gil, and Y.-O. Lee, "Validation of an ENDF/B-VII.0-based neutron and photon shielding library in MATXS-format," J. Korean Phys. Soc. **59**, 1199–1202 (2011).
7. M. Wielunski, T. Brall, M. Dommert *et al.*, "Electronic neutron dosimeter in high-energy neutron fields," Radiat. Meas. **114**, 12–18 (2018).
8. J. S. Choi, J. Farmer, C. Lee *et al.*, "Neutron-absorbing coatings for safe storage of fissile materials with enhanced shielding & criticality safety," in Materials Science and Technology Conference and Exhibition, MS and T'07: "Exploring Structure, Processing, and Applications Across Multiple Materials Systems," 2007.
9. B. Aygün, "High alloyed new stainless steel shielding material for gamma and fast neutron radiation," Nucl. Eng. Technol. **52**, 647–653 (2019).
10. C. J. Guembou Shouop, M. Ndontchueng Moyo, E. J. Nguelem Mekongtso *et al.*, "Radiological protection requirements with regard to cosmic ray exposure during air travel," Eur. Phys. J. Plus **135**, 438 (2020).
11. J. W. Shin, S.-W. Hong, S.-I. Bak *et al.*, "GEANT4 and PHITS simulations of the shielding of neutrons from the ^{252}Cf source," J. Korean Phys. Soc. **65**, 591–598 (2014).
12. S. A. M. Issa, H. O. Tekin, R. Elsaman *et al.*, "Radiation shielding and mechanical properties of Al_2O_3-Na_2O-B_2O_3-Bi_2O_3 glasses using MCNPX Monte Carlo code," Mater. Chem. Phys. **223**, 209–219 (2019).
13. K. Niita, N. Matsuda, Y. Iwamoto *et al.*, "PHITS overview," AIP Conf. Proc. **896**, 61 (2007).
14. T. Sato, Y. Iwamoto, S. Hashimoto *et al.*, "Features of particle and heavy ion transport code system (PHITS) version 3.02," J. Nucl. Sci. Technol. **55**(6), 684–690 (2018).
15. T. Sato, K. Niita, N. Matsuda *et al.*, "Particle and heavy ion transport code system, PHITS, version 2.52," J. Nucl. Sci. Technol. **50**(9), 913–923 (2013).
16. Y. Iwamoto, T. Sato, S. Hashimoto *et al.*, "Benchmark study of the recent version of the PHITS code," J. Nucl. Sci. Technol. **54**(5), 617–635 (2017).
17. T. Sato, K. Niita, N. Matsuda *et al.*, "Overview of the PHITS code and its application to medical physics," Prog. Nucl. Sci. Technol. **4**, 879–882 (2014).
18. L. Sihver, T. Sato, K. Gustafsson *et al.*, "An update about recent developments of the PHITS code," Adv. Space Res. **45**(7), 892–899 (2010).
19. K. Niita, N. Matsuda, Y. Iwamoto *et al.*, PHITS: Particle and Heavy Ion Transport code System, Version 2. 23. JAEA-Data/Code (2010).
20. C. J. Guembou Shouop and S. Bak, "Maze influence to radiological protection around industrial radiographic sources (Co-60) under 100 Ci," in *Transactions of the Korean Nuclear Society Autumn Meeting Goyang, Korea, October 24–25, 2019* (Korean Nuclear Society, 2019), pp. 3–6.
21. T. Sato, K. Niita, N. Matsuda *et al.*, "Overview of particle and heavy ion transport code system PHITS," Ann. Nucl. Energy **82**, 110–115 (2015).
22. C. J. Guembou Shouop, Shielding Design and Safety Measures Around ^{60}Co, ^{192}Ir, and ^{252}Cf Sources in Industrial Radiography Facilities Based on PHITS Monte Carlo Simulations, KAIST—Korea Advanced Institute of Science and Technology, 2020.
23. G. Shouop, C. Joel, N. M. Maurice *et al.*, "Monte Carlo method for gamma spectrometry based on GEANT4 toolkit: Efficiency calibration of BE6530 detector," J. Environ. Radioact. **189**, 109–119 (2018).
24. K. Niita, T. Sato, H. Iwase *et al.*, "PHITS-a particle and heavy ion transport code system," Radiat. Meas. **41**(9-10), 1080–1090 (2006).